Molecular Diversity (2022) 26:3241–3254
https://doi.org/10.1007/s11030-022-10385-w

ORIGINAL ARTICLE

Azomethine-clubbed thiazoles as human tissue non-specific alkaline phosphatase (*h*-TNAP) and intestinal alkaline phosphatase (*h*-IAP) Inhibitors: kinetics and molecular docking studies

Aamer Saeed[1] · Memona Javaid[1] · Syed Jawad Ali Shah[3] · Pervaiz Ali Channar[1] · Ghulam Shabir[1] · Arfa Tehzeeb[2] · Jamshed Iqbal[3]

Received: 22 August 2021 / Accepted: 24 December 2021 / Published online: 26 January 2022

Abstract

Thiazole derivatives are known inhibitors of alkaline phosphatase, but various side effects have reduced their curative efficacy. Conversely, compounds bearing azomethine linkage display a broad spectrum of biological applications. Therefore, combining the two scaffolds in a single structural unit should result in joint beneficial effects of both. A new series of azomethine-clubbed thiazoles (**3a–i**) was synthesized and appraised for their inhibitory potential against human tissue non-specific alkaline phosphatase (*h*-TNAP) and human intestinal alkaline phosphatase (*h*-IAP). Compounds **3c** and **3f** were found to be most potent compounds toward *h*-TNAP with IC_{50} values of 0.15 ± 0.01 and 0.50 ± 0.01 µM, respectively, whereas **3a** and **3f** exhibited maximum potency for *h*-IAP with IC_{50} value of 2.59 ± 0.04 and 2.56 ± 0.02 µM, respectively. Molecular docking studies were also performed to find the type of binding interaction between potential inhibitor and active sites of enzymes. The enzymes inhibition kinetics studies were carried out to define the mechanism of enzyme inhibition. The current study leads to discovery of some potent inhibitors of alkaline phosphatase that is promising toward identification of compounds with druggable properties.

✉ Aamer Saeed
aamersaeed@yahoo.com; asaeed@qau.edu.pk

[1] Department of Chemistry, Quaid-I-Azam University, Islamabad 45320, Pakistan

[2] Department of Pharmacy, Quaid-I-Azam University, Islamabad 45320, Pakistan

[3] Centre for Advanced Drug Research, COMSATS University Islamabad, Abbottabad Campus, Abbottabad 22060, Pakistan

Graphical abstract

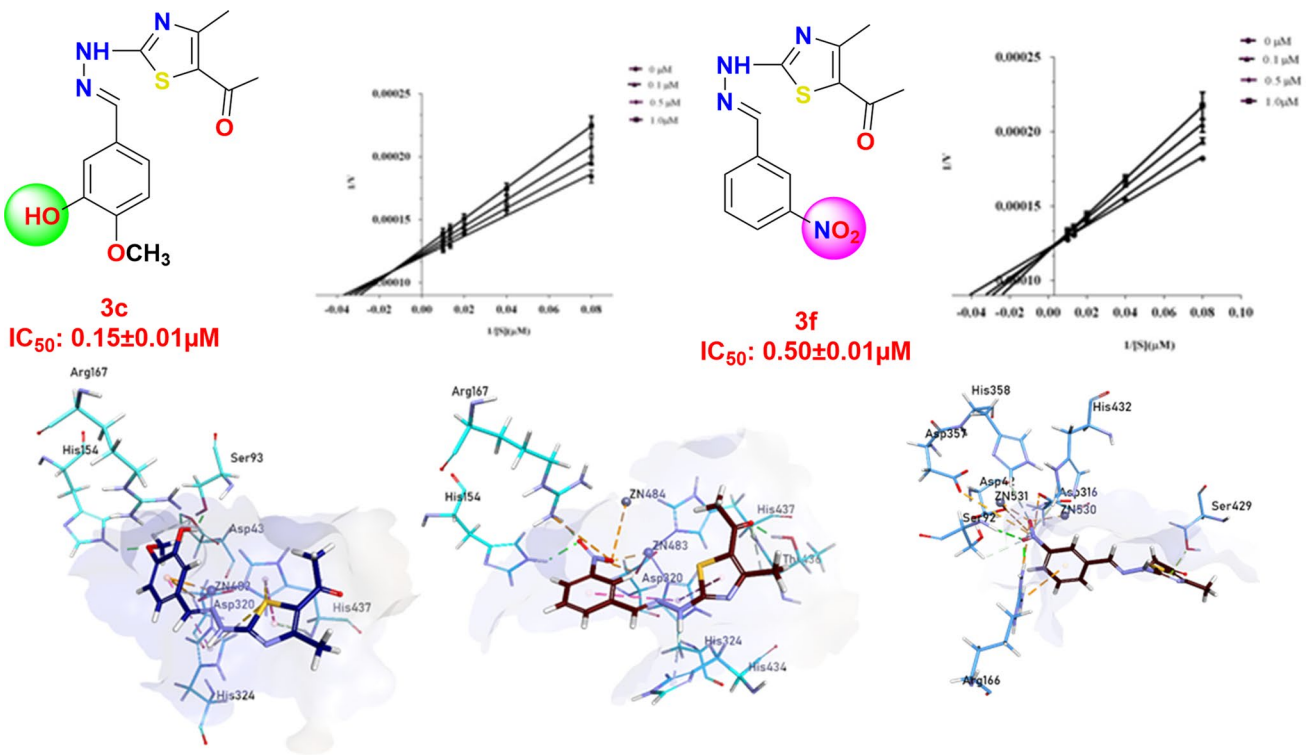

Keywords Azomethine-thiazoles · *h*-TNAP · *h*-IAP · Inhibition kinetics · Molecular docking studies

Introduction

Alkaline phosphatase (ALPs, E.C. 3.1.3.1) belongs to a family of ectonucleotidases that catalyze the dephosphorylation of nucleosides into corresponding nucleotides. These are metalloenzymes with two Zn^{2+} and one Mg^{2+} ions in their active site for optimum activity [1]. Elevated serum level of alkaline phosphatase is an indication of liver and bone diseases such as Paget's disease, hyperparathyroidism, vitamin D deficiency, damaged liver cells and celiac disease [2, 3]. Reduced ALP serum level may also be observed in several other pathophysiological states like hypophosphatasia, recent heart surgery, hypothyroidism, malnutrition, severe anemia, aplastic anemia, pernicious anemia, myelogenous leukemia and Wilson's disease. Deficiency of TNAP has been found to cause hypophosphatasia in infants that results in epileptic seizure. Moreover, this deficiency also causes hypo-mineralization of teeth and bones [4].

In human genome, four genes are known to be involved in expression of these enzymes, categorized as tissue specific (TSAP) and tissue non-specific alkaline phosphatase (TNAP). The former includes intestinal alkaline phosphatase (IAP), placental alkaline phosphatase (PALP) and germ cells alkaline phosphatase (GCALP). However, TNAP is one of the four isozymes in humans that can hydrolyze phosphate groups of wide variety of biological substrates. TNAP is post-transnationally modified to bone, kidney and liver isoforms [5]. Hypophosphatasia leads to alteration of pyridoxal 5′-phosphate, pyrophosphate and phosphoethanolamine metabolism indicating the significance of alkaline phosphatase [6].

Overexpression of ALP is found to be in association with several human cancers [7, 8]. Higher tissue non-specific alkaline phosphatase level induces carbonate-substituted hydroxyapatite crystal deposition that leads to osteoarthritis; therefore, inhibition of TNAP is an auspicious way to treat rheumatoid arthritis [9, 10]. Levamisole and tetramisole containing azole ring are recognized inhibitors of TNAP but cause skin rashes and agranulocytosis that limit their therapeutic effectiveness [11].

Thiazole moiety is a heart core of various commercially available drugs and are in current clinical practices. Thiazole containing molecules are known to possess diverse biological activities including anticancer, antimicrobial, anti-inflammatory, antioxidant and anti-tubercular activities [12, 13]. Also, various azomethine derivatives exhibit antioxidant, antimicrobial, anticancer and antimalarial activities [14–16] (Fig. 1). In current study, both distinctive chemical

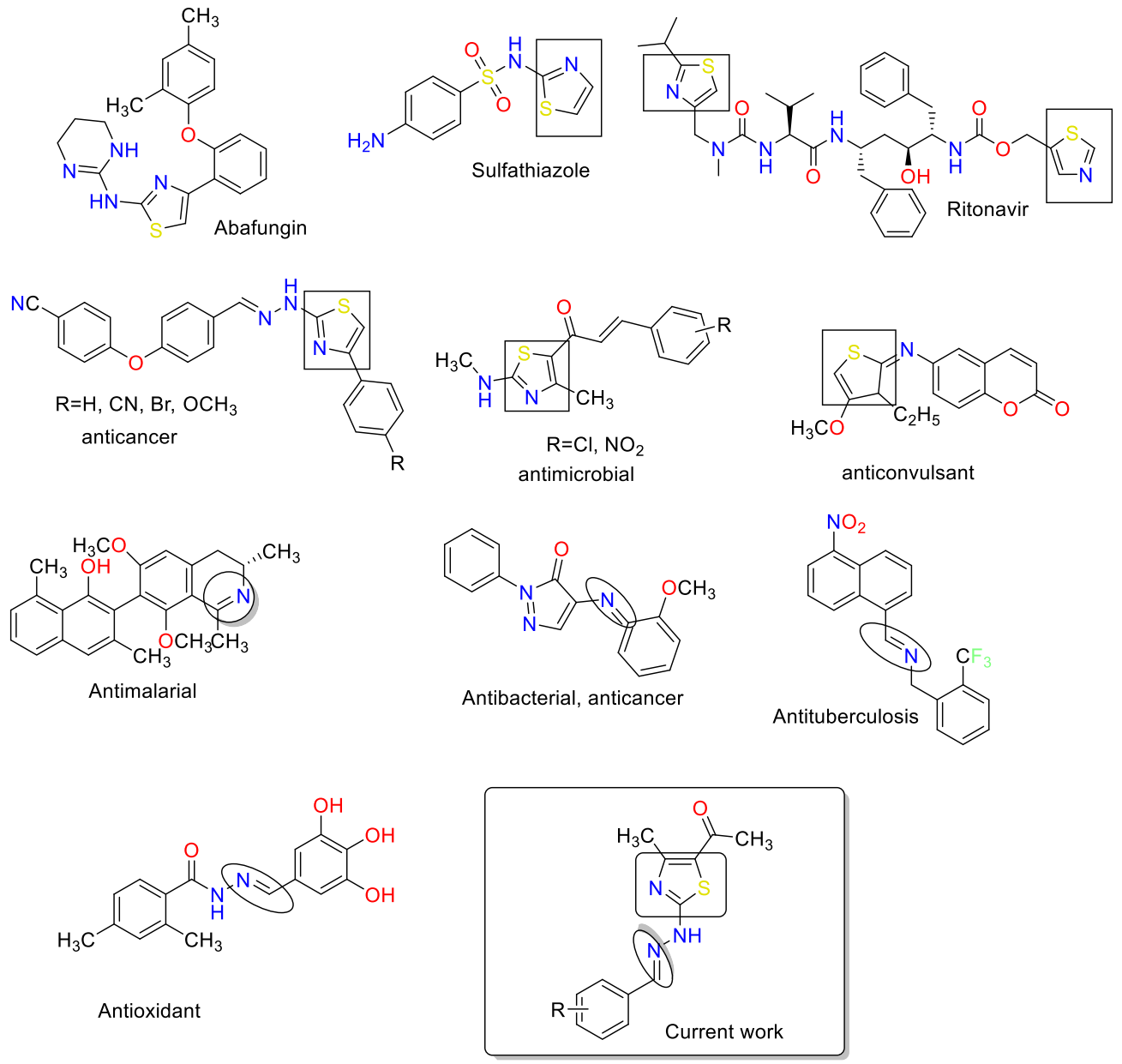

Fig. 1 Some literature reported bioactive thiazole and azomethine compounds and structural architecture of current work

moieties are gathered in single scaffold to find potent and selective inhibitors of alkaline phosphatases.

Experimental

All the chemicals and solvents used were acquired from the standard source (Sigma-Aldrich and Merck). Distillation of solvents and starting materials was carried out by using standard procedures. Melting point was determined on Gallenkamp melting point apparatus. ^{1}H and ^{13}C NMR spectra were recorded on Bruker AM-300 spectrophotometer using $CDCl_3$) as solvent. Thin layer chromatography was carried out on pre-coated silica gel plates that observe the UV to check the progress of reaction.

General procedure for the synthesis of azomethine-thiazole hybrids (3a–i)

Suitably substituted aromatic aldehyde (1.0 mmol) was added to dry ethanol (15 mL) in a two-neck round bottom flask fitted with reflux condenser and stirred for 5 min. A solution of thiosemicarbazide (1.0 mmol) in dry ethanol (20 mL) was added dropwise. The resulting mixture was

heated at reflux for 3–4 h. After accomplishment of reaction (TLC), the products precipitated out which were purified by recrystallization in acetone and ethanol to afford azomethine (**2a–j**).

Azomethines (**2a–j**) (1.0 mmol) were taken in the round bottom flask containing in 25 ml dry ethanol. A solution of 3-chloroacetyl acetone (1.0 mmol) in dry ethanol was added. The reaction mixture was refluxed for 18–20 h the completion of reaction as monitored by TLC. The solid precipitated out was filtered and purified by recrystallization in ethanol to yield the azomethine-thiazole hybrids (**3a–i**).

(*E*)-1-(2-(2-((2-Hydroxynaphthalen-1-yl)methylene) hydrazineyl)-4-methylthiazol-5-yl)ethan-1-one (3a)

Yield = 77%; Yellowish powder; M.P = 294–295 °C; R_f = 0.55 (methanol: chloroform, 1:9); FT-IR (ATR) in cm^{-1}, 3162 (H–N), 2920 (H–C, Ar), 1696 (C=O), 1583 (C=N, imine), 1496 (C = C, Ar); ^{1}H-NMR (300 MHz, $CDCl_3$); in δ (ppm), 12.4 (s, 1H, OH), 11.7 (s, 1H, N–H), 9.14 (s, 1H, imine), 8.62 (d, 1H, *J* = 6.9 Hz, naphthyl-H), 7.91–7.36 (m, 4H, naphthyl-H), 7.23 (d, 1H, *J* = 6.9 Hz, naphthyl-H), 2.49 (s, 3H, CH_3), 2.41(s, 3H, CH_3); ^{13}C-NMR (75 MHz, $CDCl_3$) in δ (ppm), 189.0 (acetyl, C=O), 158.0 (thiazole, C=N), 133.0 (imine, C), 131.7, 129.2, 128.4, 128.2, 123.9, 123.76, 122.9, 122.8, 119.05, 119.7, 118.8, 110.0, 29.6, 17.2. Anal. Calcd. for $C_{17}H_{15}N_3O_2S$ C, 62.7; H, 4.65; N, 12.91; S, 9.85, found; C, 62.79; H, 4.68; N, 12.95; S, 9.87.

(*E*)-1-(2-(2-(4-Methoxybenzylidene) hydrazinyl)-4-methylthiazol-5-yl)ethanone (3b)

Yield = 72%; Dark brown powder; M.P = 192–194 °C; R_f = 0.51 (methanol: chloroform, 1:9); FT-IR (ATR) in cm^{-1}, 3136 (H–N), 2980 (H–C, Ar), 1667 (C=O), 1585 (C=N, imine), 1467 (C = C, Ar); ^{1}H-NMR (300 MHz, $CDCl_3$); in δ (ppm), 11.89 (s, 1H, N–H), 8.41 (s, 1H, imine), 7.62 (d, 2H, *J* = 8.1 Hz, phenyl-H), 7.23 (d, 2H, *J* = 8.1 Hz, phenyl-H), 3.73 (s, 3H, methoxy-H), 2.49 (s, 3H, CH_3), 2.41(s, 3H, CH_3); ^{13}C-NMR (75 MHz, $CDCl_3$) in δ (ppm), 180.0 (acetyl, C=O), 168.1 (thiazole, C=N), 135.1 (imine, C), 130.3, 128.2, 128.4, 123.7, 119.7, 118.8, 65.8, 56.4 (OMe), 29.6, 17.2. Anal. Calcd. for $C_{14}H_{15}N_3O_2S$ C, 58.11; H, 5.23; N, 14.52; S, 11.08 found; C, 58.14; H, 5.26; N, 14.55; S, 11.12.

(*E*)-1-(2-(2-(3-Hydroxy-4-methoxybenzylidene) hydrazineyl)-4-methylthiazol-5-yl)ethan-1-one (3c)

Yield = 73%; Brown powder; M.P = 239–240 °C; R_f = 0.61 (methanol: chloroform, 1:9); FT-IR (ATR) in cm^{-1}, 3222 (H–N), 3019 (H–C, Ar), 1709 (C=O), 1566 (C=N, imine), 1536 (C = C, Ar); ^{1}H-NMR (300 MHz, $CDCl_3$); in δ (ppm), 12.71 (s, 1H, OH), 11.89 (s, 1H, N–H), 9.65 (s, 1H, imine), 7.72 (d, 1H, *J* = 6.9 Hz, phenyl-H), 7.36 (s, 1H, phenyl-H), 7.27 (d, 1H, *J* = 6.9 Hz, phenyl-H), 3.67 (s, 3H, methoxy-H), 2.51 (s, 3H, CH_3), 2.47(s, 3H, CH_3); ^{13}C-NMR (75 MHz, $CDCl_3$) δ (ppm), 179.6 (acetyl, C=O), 155.7 (thiazole, C=N), 135.6 (imine, C), 131.7, 129.2, 128.2, 123.9, 123.7, 122.9, 122.8, 119.0, 56.3 (OMe), 68.7, 30.6, 19.2. Anal. Calcd. for $C_{14}H_{15}N_3O_3S$, C, 55.07; H, 4.95; N, 13.76; S, 10.50 found; C, 55.09; H, 4.98; N, 13.79; S, 10.55.

(*E*)-1-(2-(2-Benzylidenehydrazineyl)-4-methylthiazol-5-yl) ethan-1-one (3d)

Yield = 83%; Light green powder; M.P = 266–268 °C; R_f = 0.55 (ethyl acetate: *n*-hexane, 4:6); FT-IR (ATR) in cm^{-1}, 3120 (H–N), 2960 (H–C, Ar), 1715 (C=O), 1578 (C=N, imine), 1484 (C = C, Ar); ^{1}H-NMR (300 MHz, $CDCl_3$); in δ (ppm), 11.71 (s, 1H, N–H), 9.75 (s, 1H, imine), 7.66 (m, 4H, phenyl-H), 2.43 (s, 3H, CH_3), 2.33 (s, 3H, CH_3); ^{13}C-NMR (75 MHz, $CDCl_3$) in δ (ppm), 180.0 (acetyl, C=O), 165.0 (thiazole, C=N), 136.3 (imine, C), 130.3, 128.7, 128.2, 123.9, 123.76, 122.9, 122.8, 33.1, 18.0. Anal. Calcd. for $C_{13}H_{13}N_3O_2S$, C, 56.71; H, 4.76; N, 15.26; S, 11.65, found; C, 56.73; H, 4.79; N, 15.29; S, 11.68.

(*E*)-1-(4-Methyl-2-(2-(4-nitrobenzylidene)hydrazineyl) thiazol-5-yl)ethan-1-one (3e)

Yield = 86%; Light orange powder; M.P = 286–287 °C; R_f = 0.53 (ethyl acetate: *n*-hexane, 4:6); FT-IR (ATR) in cm^{-1}, 3122 (H–N), 2990 (H–C, Ar), 1697 (C=O), 1580 (C=N, imine), 1517 (C = C, Ar); ^{1}H-NMR (300 MHz, $CDCl_3$); in δ (ppm), 12.09 (s, 1H, N–H), 8.41 (s, 1H, imine), 7.52 (d, 2H, *J* = 8.1 Hz, phenyl-H), 7.23 (d, 2H, *J* = 8.1 Hz, phenyl-H), 2.62 (s, 3H, CH_3), 2.51(s, 3H, CH_3); ^{13}C-NMR (75 MHz, $CDCl_3$) in δ (ppm), 175.0 (acetyl, C=O), 160.1 (thiazole, C=N), 151.3, 138.0 (imine, C), 130.3, 129.0, 128.4, 124.5, 120.7, 118.5, 30.1, 18.4. Anal. Calcd. for $C_{13}H_{12}N_4O_3S$, C, 51.31; H, 3.97; N, 18.41; S, 10.54, found; C, 51.34; H, 3.99; N, 18.46; S, 10.57.

(*E*)-1-(4-Methyl-2-(2-(3-nitrobenzylidene)hydrazineyl) thiazol-5-yl)ethan-1-one (3f)

Yield = 77%; Yellow powder; M.P = 262–264 °C; R_f = 0.57 (ethyl acetate: *n*-hexane, 4:6); FT-IR (ATR) in cm^{-1}, 3204 (H–N), 2980 (H–C, Ar), 1703 (C=O), 1588 (C=N, imine), 1489 (C = C, Ar); ^{1}H-NMR (300 MHz, $CDCl_3$); in δ (ppm), 11.34 (s, 1H, N–H), 8.63 (s, 1H, imine), 7.77 (t, 1H, *J* = 6.3 Hz, phenyl-H), 7.61 (s, 1H, phenyl-H), 7.23 (d, 1H, *J* = 6.3 Hz, phenyl-H), 7.11 (d, 1H, *J* = 6.3 Hz, phenyl-H),2.77 (s, 3H, CH_3), 2.63(s, 3H, CH_3); ^{13}C-NMR (75 MHz, $CDCl_3$) in δ (ppm), 172.1 (acetyl, C=O), 163.3 (thiazole, C=N), 160.6, 135.1 (imine, C), 147.3, 130.6, 130,1, 129.09,

128.9, 125.6, 124.6, 120.7, 118.5, 31.1, 17.6. Anal. Calcd. for $C_{13}H_{12}N_4O_3S$, C, 51.31; H, 3.97; N, 18.41; S, 10.54, found; C, 51.36; H, 3.99; N, 18.45; S, 10.56.

(*E*)-1-(2-(2-(4-Hydroxybenzylidene) hydrazineyl)-4-methylthiazol-5-yl)ethan-1-one (3g)

Yield = 82%; Light green powder; M.P = 297–298 °C; R_f = 0.53 (ethyl acetate: *n*-hexane, 4:6); FT-IR (ATR) in cm^{-1}, 3123 (H–N), 2985 (H–C, Ar), 1687 (C=O), 1605 (C=N, imine), 1509 (C = C, Ar); ^{1}H-NMR (300 MHz, $CDCl_3$); in δ (ppm), 12.74 (s, 1H, OH), 11.53 (s, 1H, N–H), 8.19 (s, 1H, imine), 7.66 (d, 2H, *J* = 8.1 Hz, phenyl-H), 7.39 (d, 2H, *J* = 8.1 Hz, phenyl-H), 2.88 (s, 3H, CH_3), 2.61(s, 3H, CH_3); ^{13}C-NMR (75 MHz, $CDCl_3$) δ (ppm); 178.1 (acetyl, C=O), 164.1 (thiazole, C=N), 160.2, 135.6 (imine, C), 130.3, 129.0, 128.8, 124.7, 120.7, 119.5, 30.5, 17.1. Anal. Calcd. for $C_{13}H_{13}N_3O_2S$ C, 56.71; H, 4.76; N, 15.26; S, 11.65, found; C, 56.74; H, 4.78; N, 15.29; S, 11.68.

(*E*)-1-(2-(2-(4-(Ethynyl(methyl)amino)benzylidene) hydrazineyl)-4-methylthiazol-5-yl)ethan-1-one (3h)

Yield = 86%; Green powder; M.P = 255–256 °C; R_f = 0.61 (methanol: chloroform, 1:9); FT-IR (ATR) in cm^{-1}, 3122 (H–N), 2988 (H–C, Ar), 1670 (C=O), 1577 (C=N, imine), 1496 (C = C, Ar); ^{1}H-NMR (300 MHz, $CDCl_3$); in δ (ppm), 11.53 (s, 1H, N–H), 8.63 (s, 1H, imine), 7.69 (d, 2H, *J* = 8.1 Hz, phenyl-H), 7.57 (d, 2H, *J* = 8.1 Hz, phenyl-H), 2.88(s, 3H, CH_3), 2.71(s, 3H, CH_3), 2.60(s, 3H, CH_3), 1.8 (s, 1H, CH); ^{13}C-NMR (75 MHz, $CDCl_3$) in δ (ppm), 179.1 (acetyl, C=O), 171.8, 167.1 (thiazole, C=N), 139.6 (imine, C), 130.3, 129.0, 128.8, 125.7, 120.78, 119.5, 81.51 72.78, 67.6, 40.1, 30.5, 17.1. Anal. Calcd. for $C_{16}H_{16}N_4OS$ C, 61.52; H, 5.16; N, 17.93; S, 10.26, found; C, 61.55; H, 5.18; N, 17.96; S, 10.27.

(*E*)-1-(2-(2-(3,4,5-Trimethoxybenzylidene) hydrazineyl)-4-methylthiazol-5-yl)ethan-1-one (3i)

Yield = 77%; Light green powder; M.P = 247–248 °C; R_f = 0.41(ethyl acetate: *n*-hexane, 4:6); FT-IR (ATR) in cm^{-1}, 3130 (H–N), 2977 (H–C, Ar), 1698 (C=O), 1587 (C=N, imine), 1513 (C = C, Ar); ^{1}H-NMR (300 MHz, $CDCl_3$); in δ (ppm), 12.19 (s, 1H, N–H), 8.72 (s, 1H, imine), 7.77 (s, 1H, phenyl-H), 7.22 (s, 1H, phenyl-H), 3.73(s, 9H, methoxy), 2.47 (s, 3H, CH_3), 2.44 (s, 3H, CH_3); ^{13}C-NMR (75 MHz, $CDCl_3$) in δ (ppm), 176.0 (acetyl, C=O), 165.1 (thiazole, C=N), 136. (imine, C), 130.3, 128.9, 128.8, 123.7, 121.7, 119.9, 56.50, 56.4, 23.6, 15.1. Anal. Calcd. for $C_{16}H_{19}N_3O_4S$ C, 55.00; H, 5.48; N, 12.03; S, 9.18 found; C, 55.04; H, 5.52; N, 12.07; S, 9.20.

Materials and methods

Transfection

COS-7 cells were used for transfection of *h*-TNAP and *h*-IAP proteins. When COS-7 cells reached to confluency level of 80–90%, serum-free DMEM (Dulbecco's modified Eagle's medium) containing 6 µg of plasmid and Lipofectamine (transfecting reagent) was added. Cells along with transfection mixture were incubated for 48–72 h at 37 °C in 5% CO_2 incubator. After that, transfection mixture was replaced with normal growth medium. Transfected cells were washed with cold Tris-buffer saline and centrifuged the cells at 30*g*, at 4 °C for 5 min. Cells were washed with same ice cold buffer, and were resuspended in 10 µg/mL aprotinin. Protein was quantified and preserved in 7.5% glycerol and stored at −80 °C [17, 18].

Enzyme inhibition assay

Inhibitory potentials of thiazole derivatives were analyzed by using CDP-Star®(disodium 2-chloro-5-(4-methoxyspiro[1,2-dioxetane-3,20-(5-chlorotricyclo[3.3.1.13.7]decan])-4-yl]-1-phenyl phosphate) that is a chemiluminescent substrate. The inhibitory assay was performed after slight modification in previously reported spectrophotometric method [19]. Working enzymes were made in DEA (250 mM) buffer containing 0.005 mM $ZnCl_2$ and 2.5 mM $MgCl_2$. The working solutions of enzymes were 5 and 3.335 µg/mL for *h*-TNAP and *h*-IAP, respectively. Assay was preceded by adding 20 µL of enzyme followed by 10 µL of potential inhibitor in each well of 384 wells white plate. The final concentration of inhibitor in assay volume was 0.2 M. The assay mixture was incubated for 10 min at 37 °C. The reaction was started by addition of 20 µL of CDP-Star® in each well with final concentration of 105.2 and 177 µM for *h*-TNAP and *h*-IAP, respectively. Luminescence was measured at 0 min and second read was taken after 10 min of incubation by using microplate reader (BioTek FLx800, Instruments, Inc. USA). The activity of each inhibitor was compared with negative control (without any inhibitor). Inhibition potential of each compound was measured by following mentioned formula. Compounds exhibiting inhibition more than 50% were further investigated for IC_{50} values. All experiments were performed in triplicate format. PRISM 5.0 (GraphPad, San Diego, California, USA) was used for non-linear regression analysis for dose response curve and IC_{50} value determination [19].

Enzyme kinetics studies

Enzyme kinetics studies were performed to find out the mode of enzyme inhibition. Compounds **3c** and **3f** were

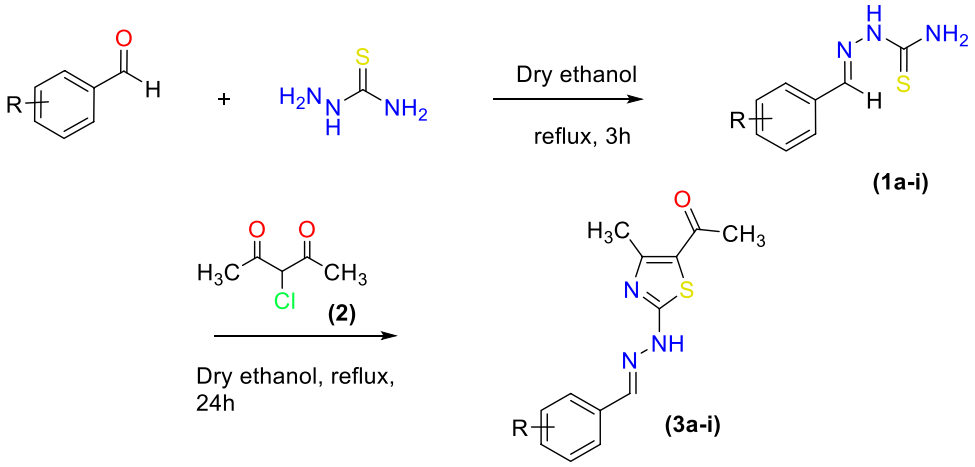

Scheme 1 Synthetic pathway to (*E*)-1-(2-(2-((aryl)methylene) hydrazineyl)-4-methylthiazol-5-yl)ethan-1-ones (**3a–i**)

selected for *h*-TNAP, as both the compounds were found to be most potent among the tested series. Both the compounds were used at concentration of 0, 0.1, 0.5 and 1 µM, whereas the compound **3f** was used for enzyme kinetic study toward *h*-IAP. Here, the used compound concentrations were 0, 1.5, 3.0 and 6.0 µM. For all these mentioned compounds, the used CDP-Star substrate concentrations were 0, 12.5, 25, 50 and 100 µM.

Selection of the protein structures and preparation of ligands

Crystallographic structures of *h*-TNAP and *h*-IAP are not available; thus, homology modeled structures of *h*-TNAP and *h*-IAP were employed for molecular docking studies. The proteins and ligands were prepared prior to molecular docking studies using Molecular Operating Environment (MOE) [21]. *h*-TNAP and *h*-IAP models binding validation was done with the positive standards, Levamisole for *h*-TNAP and L-phenylalanine for *h*-IAP, used in the in vitro analysis. MOE site finder was used for the selections of binding site of these receptors, keeping the catalytic zinc ions in the center of the active site. After initial validation, molecular docking of the selected ligands was carried out [20].

Docking experiment

The homology models of *h*-TNAP and *h*-IAP previously reported were used without any alternation and modification to identify the putative binding modes of the inhibitors [21]. Molecular docking studies were performed on LeadIT (BioSolveIT GmbH, Germany) [22] through default parameters, for the selected compounds as well as the reference standards (used in *in vitro* assay). The most promising docked pose was selected for each ligand, and it was further analyzed by the HYDE assessment tool. The 3D interactions of the poses were examined using Discovery Studio Visualizer [23].

Results and discussion

Azomethine-clubbed thiazole were synthesized according to the route shown in Scheme 1. The first step involved the reaction of suitably substituted benzaldehydes with thiosemicarbazide in dry ethanol to afford azomethines intermediates (**1a–i**). Heterocyclization of azomethines (**1a–i**) with 3-chloroacetyl acetone (**2**) furnished the desired azomethine-thiazoles (**3a–i**) in good to excellent percentage yield and in high purity.

Figure 2 shows the complete molecular structures of the synthesized azomethine-thiazole derivatives **(3a–i)** along with their percent yields.

The FT-IR analysis revealed the characteristic absorptions for N–H at 3222–3103 cm^{-1}, C–H aromatic at 2960–3019 cm^{-1}, C=O at 1667–1715 cm^{-1} and C=N at 1566–1605 cm^{-1}. In a typical case of **3a**, ^{1}H-NMR shows singlets at δ 12.44 for OH, at δ 11.71 for N–H, at 9.14 for imine proton, besides signals at for methyl of thiazole ring at 2.49, besides the methyl of acetyl group at δ 2.41. The aromatic protons appeared in the range of 7.91–7.23 ppm. ^{13}C-NMR signals at δ 189.0 corresponded to acetyl carbonyl, that 179.0 to C=N of thiazole, 133.0 for ipso carbon attached to acetyl. Similarly, the methyl carbons of thiazole ring and acetyl resonated at 29.6 and 17.24, respectively.

Inhibitory potential of azomethine-thiazoles for alkaline phosphatases and Structure Activity Relationship (SAR)

All the synthesized thiazole derivatives were analyzed for inhibitory potential toward *h*-TNAP and *h*-IAP and results are listed in Table 1.

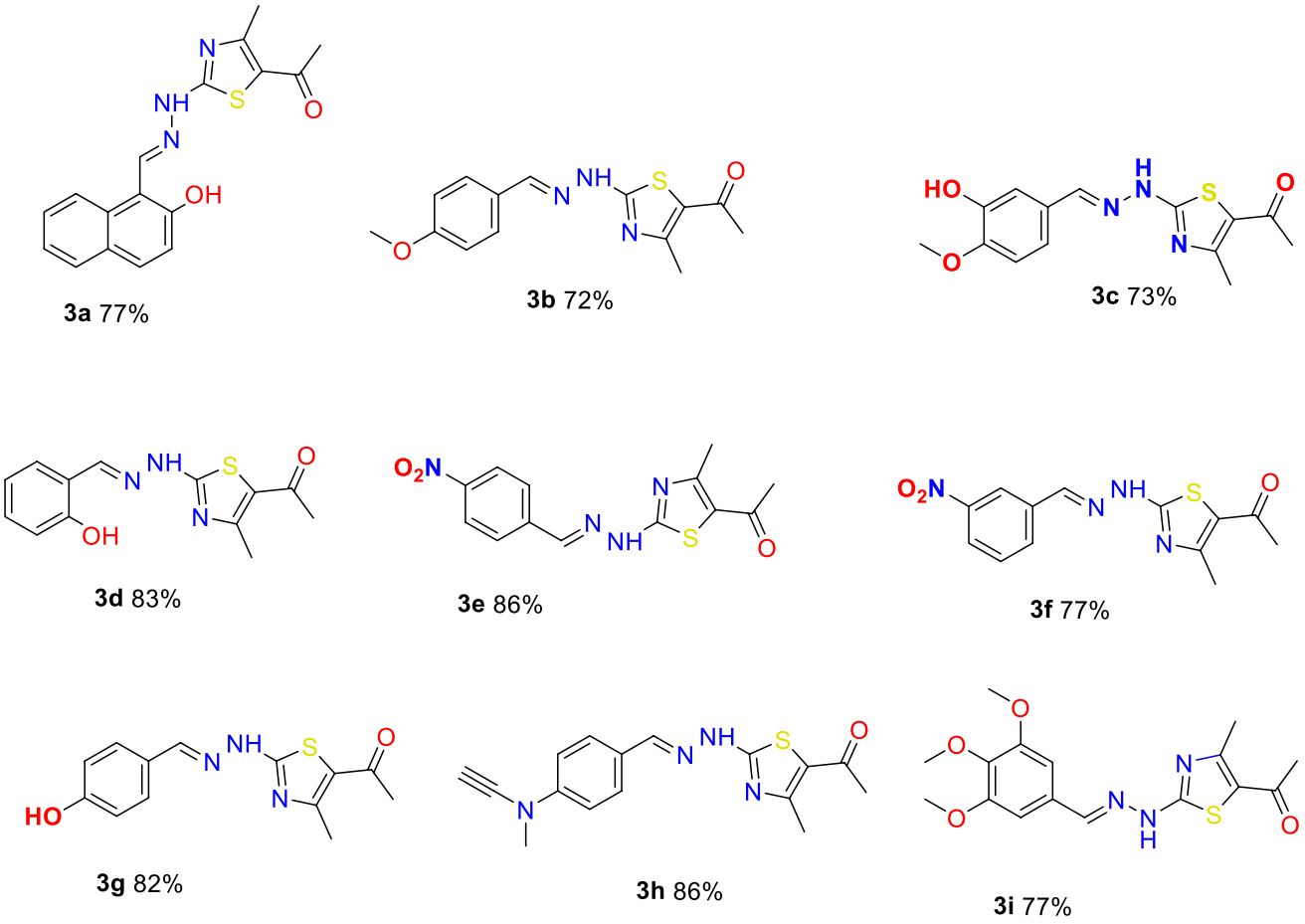

Fig. 2 Chemical structures of new azomethine-clubbed thiazoles **(3a–i)**

Table 1 Inhibitory potential of thiazole derivatives for *h*-TNAP and *h*-IAP

Compound	*h*-TNAP $IC_{50} \pm SEM$ (μM)/%Inhibition	*h*-IAP $IC_{50} \pm SEM$ (μM)/%Inhibition
3a	5.82 ± 0.03	2.59 ± 0.04
3b	2.19 ± 0.01	4.52 ± 0.02
3c	0.15 ± 0.01	7.9 ± 0.03
3d	3.47 ± 0.03	6.91 ± 0.1
3e	12.30 ± 0.3	6.05 ± 0.1
3f	0.50 ± 0.01	2.56 ± 0.02
3g	1.73 ± 0.03	5.92 ± 0.1
3h	3.01 ± 0.02	5.21 ± 0.09
3i	8.37 ± 0.1	7.94 ± 0.2
Levamisole	25.2 ± 1.9	–
L-phenylalanine	–	100 ± 3.0

The results indicated that all derivatives are inhibitors of both isozymes of alkaline phosphatases. Compounds **3c** and **3f** were found to most potent for *h*-TNAP with IC_{50} value of 0.15 ± 0.01 and 0.50 ± 0.01 μM with potency is much higher than standard Levamisole (IC_{50} of 25.2 ± 1.9 μM) and is also evident from the molecular docking scores (i.e., −17.65 and −21.02 for compounds **3c** and **3f** against −12.02 for levamisole). The presence of 3-hydroxy-4-methoxybenzylidene in **3c** results in most potent inhibitor of TNAP. Removal of 3-hydroxyl group in **3b** leads to decrease in inhibitory potential for *h*-TNAP that signifies the importance of hydroxyl group at position 3 of the benzene ring. The molecular basis for the hydroxyl group activity is clarified by the docking study which showed its hydrogen bonding potential with Glu315 and Arg167. Similarly, **3d** and **3g** having the hydroxyl group on positions 2 and 4, respectively, also exhibited the potent inhibition (Fig. 3). Lower binding scores of −14.09 for compound **3b** were observed against the binding scores of −14.26 and −15.74 for compounds **3d** and **3g**. Similarly, the presence of nitro (–NO_2) on phenyl ring also increases the potency about 95 times for **3e** (IC_{50}: 12.30 ± 0.3 μM and binding scores of −14.52) to **3f** (IC_{50}: 050 ± 0.01 μM and binding scores of −21.02).

For *h*-IAP, **3f** and **3a** were found to be more potent with IC_{50} values of 2.56 ± 0.02 and 2.59 ± 0.04 μM, respectively. Both inhibitors exhibited more potent activity as compared

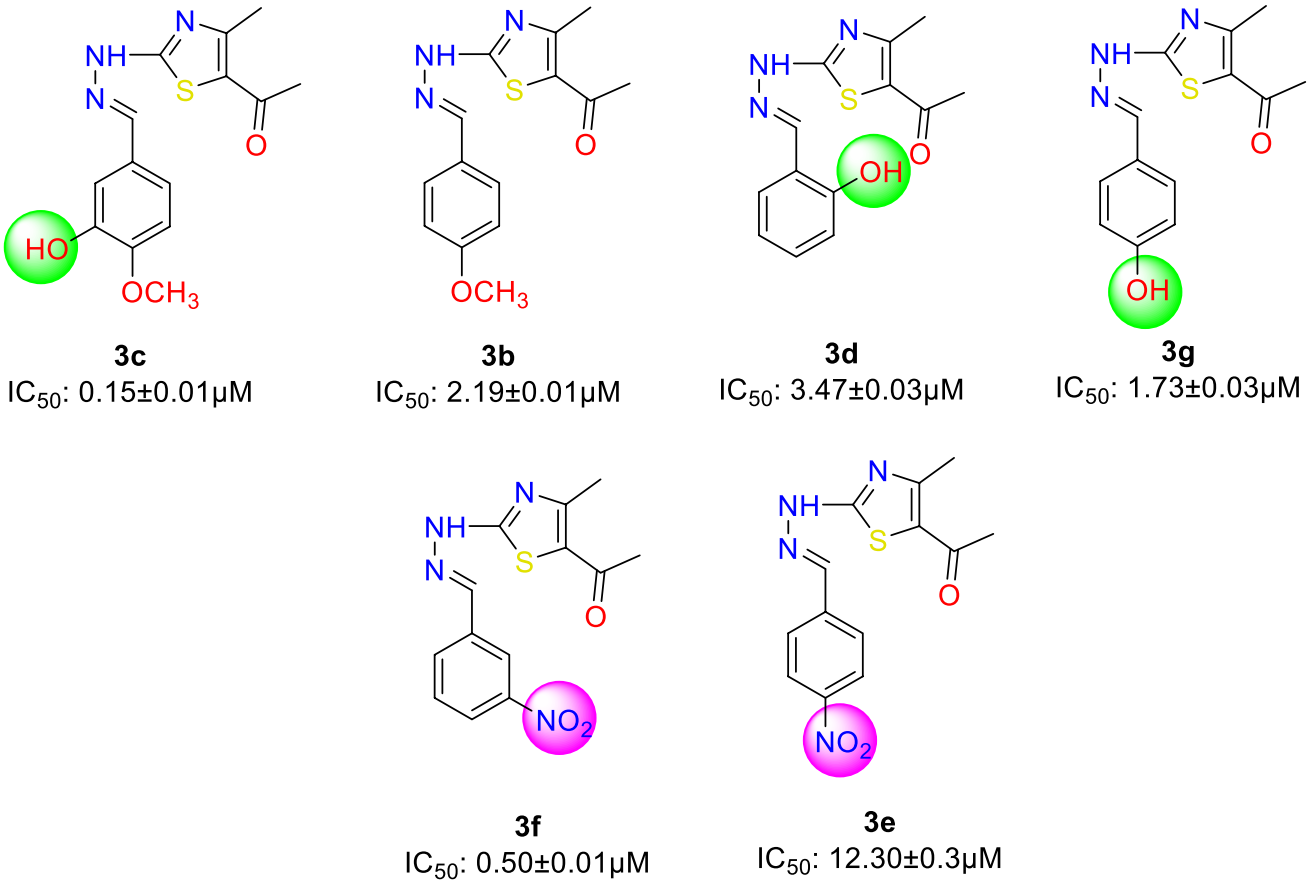

Fig. 3 Influence of hydroxyl group (–OH) and nitro group (–NO_2) substitutions on inhibitory potential of thiazole derivatives for *h*-TNAP

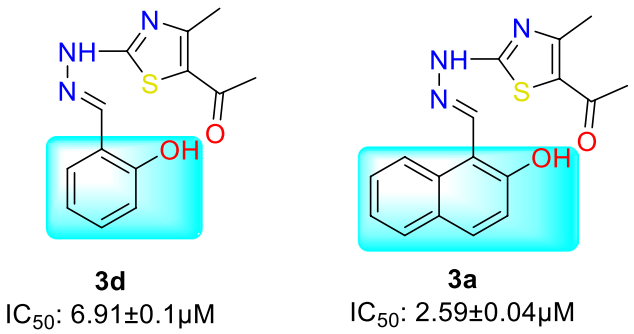

Fig. 4 Effect of substitution of aryl-ring on the inhibitory potential of thiazole derivatives for *h*-IAP

to L-phenylalanine (IC_{50}: 100 ± 3.0 μM), a positive inhibitor of *h*-IAP. Replacement of 2-hydroxyphenyl in **3d** with 2-hydroxynaphthyl in **3a** caused to increase in inhibitory potency from 6.91 ± 0.1 to 2.59 ± 0.04 μM and binding scores of −18.97 to −20.99, respectively (Fig. 4). In addition, **3f 3c** and **3g** were found to be more selective for *h*-TNAP as compared to *h*-IAP, as shown by respective IC_{50} values for both isozymes.

Enzyme Kinetics studies for *h*-TNAP and *h*-IAP

Lineweaver Burk plot was used to define the enzyme kinetic parameters of most potent inhibitors of *h*-TNAP and *h*-IAP. Compound **3c** exhibited mixed type of inhibition for *h*-TNAP. Similarly, **3f** was also analyzed for enzyme kinetic studies for both ALP isozymes. It was found that this molecule has competitive mode of inhibition for *h*-TNAP and uncompetitive mode of inhibition for *h*-IAP. Here, the used substrate concentrations were 0, 12.5, 25, 50 and 100 μM. (Fig. 5).

Molecular docking studies

Molecular docking studies against TNAP

The binding process of potent compounds in *h*-TNAP was validated through the binding mechanism of its positive control Levamisole (Fig. 6). *In vitro* analysis reckoned **3c, 3f** and **3g** as promising inhibitors of the TNAP protein. Zn^{2+}483 ion and His154 were the common residues to bind with all the selected test compounds. Ser93, Arg167

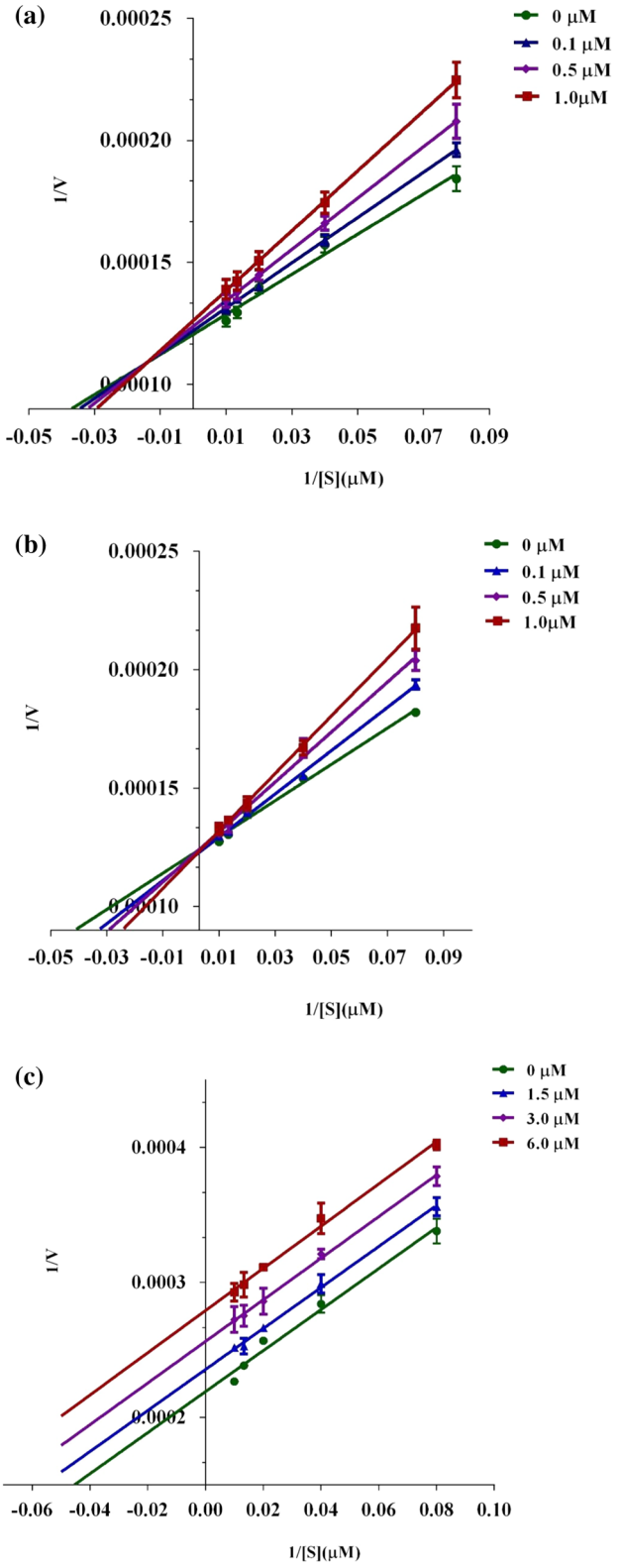

Fig. 5 Double-reciprocal plots of the inhibition kinetics of ***h*-TNAP** by compounds **3c** (**a**) exhibited mixed type of inhibition and **3f** (**b**) indicating competitive mode of inhibition. For ***h*-IAP**, **3f** exhibited uncompetitive type of inhibition (**c**)

and Asp320 were the other prominent residues to interact with the test compounds. Major interactions depicted were hydrogen bonding, π–π interactions, π–alkyl interactions and π–cation/anionic interactions between the residues and compounds. The compound **3c** showed hydrogen bonding with Asp43, Ser93, His154, Arg167 and His437 residues, along with π–cation/anionic interactions with Zn^{2+}483, Asp320 and π–sulfur interactions with His324 residue of the protein (Fig. 7). Compound **3f** exhibited hydrogen bonding with His154, His434, Thr436 and His437 residues, along with π–cation/anionic interactions with Zn^{2+}483, Zn^{2+}484, Arg167, Asp320 and π–π interactions with His324 residue of the protein (Fig. 8). Compound **3g** interacted through H-bonding with Gly317, Thr436 and His437 residues, along with π–cation/anionic interactions with Zn^{2+}483, Arg167 and π–π interactions with His154, His324 and His434 residues of the protein (Fig. 9).

Molecular docking studies for (h-IAP)

L-phenylalanine was docked into the *h*-IAP protein to find the binding site residues to validate the bindings for the test compounds. L-phenylalanine exhibited interactions with the two Zn^{2+} ions along with hydrogen bonding with Ser92, Arg166, His432 and His358 while π–π interactions with His317 and His320 residues (Fig. 10). *In vitro* analysis found **3a** and **3f** as potent inhibitors of the *h*-IAP protein, and the molecular docking provided the validation for it by imitating the interactions of L-phenylalanine. The compound **3a** showed hydrogen bonding with Ser92, His153, Arg166, Thr431 and His432 residues, along with π–cation/anionic interactions with Zn^{2+}530, Asp316 and π–sulfur interactions with His320 residue of the protein. Phe107 and His320 also exhibited π–π interactions with the compound **3a** (Fig. 11). The compound **3f** showed hydrogen bonding with Ser92, Arg166, His358 and His432 residues, along with π–cationic interactions with Zn^{2+}530, Zn^{2+}531, Arg166, Asp316, Asp357 and π–lone pair interactions with Ser429 residue of the protein (Fig. 12).

The docking score of the whole series against both isozymes was carried out and results are listed in Table 2.

Conclusions

Newly synthesized azomethine-thiazoles were evaluated for their inhibitory potential against h-TNAP and *h*-IAP. Compounds **3c** and **3f** were found to be most potent compounds toward *h*-TNAP with IC_{50} values of 0.15 ± 0.01 and 0.50 ± 0.01 µM, respectively, while **3a** and **3f** exhibited maximum potency for *h*-IAP with IC_{50} value of 2.59 ± 0.04 and 2.56 ± 0.02 µM, respectively. The compounds exhibiting high potency were also subjected to the molecular

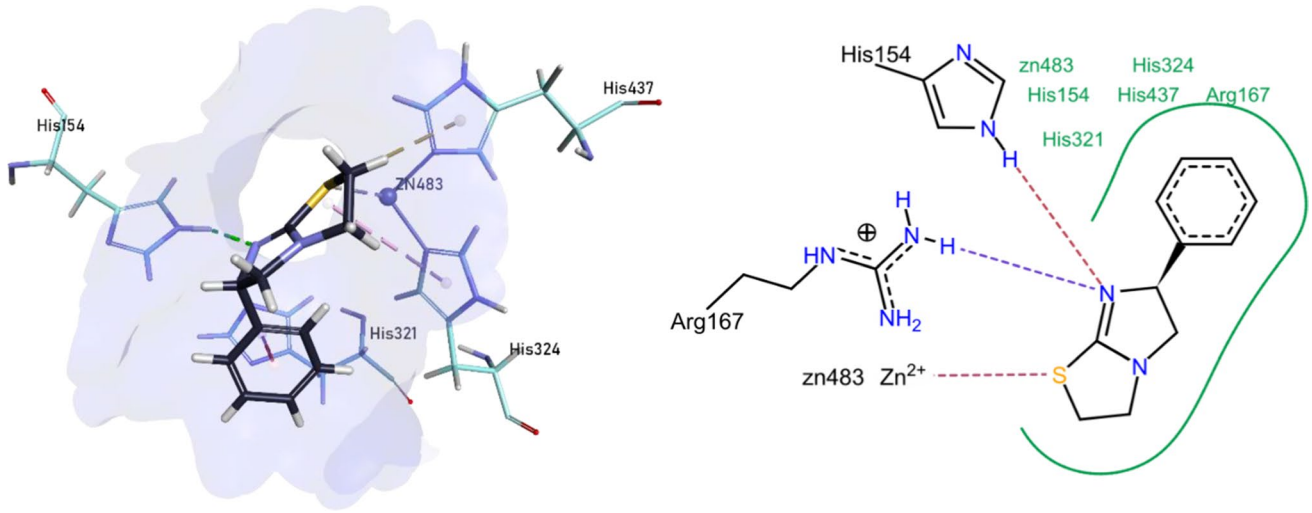

Fig. 6 Levamisole docking with h-TNAP

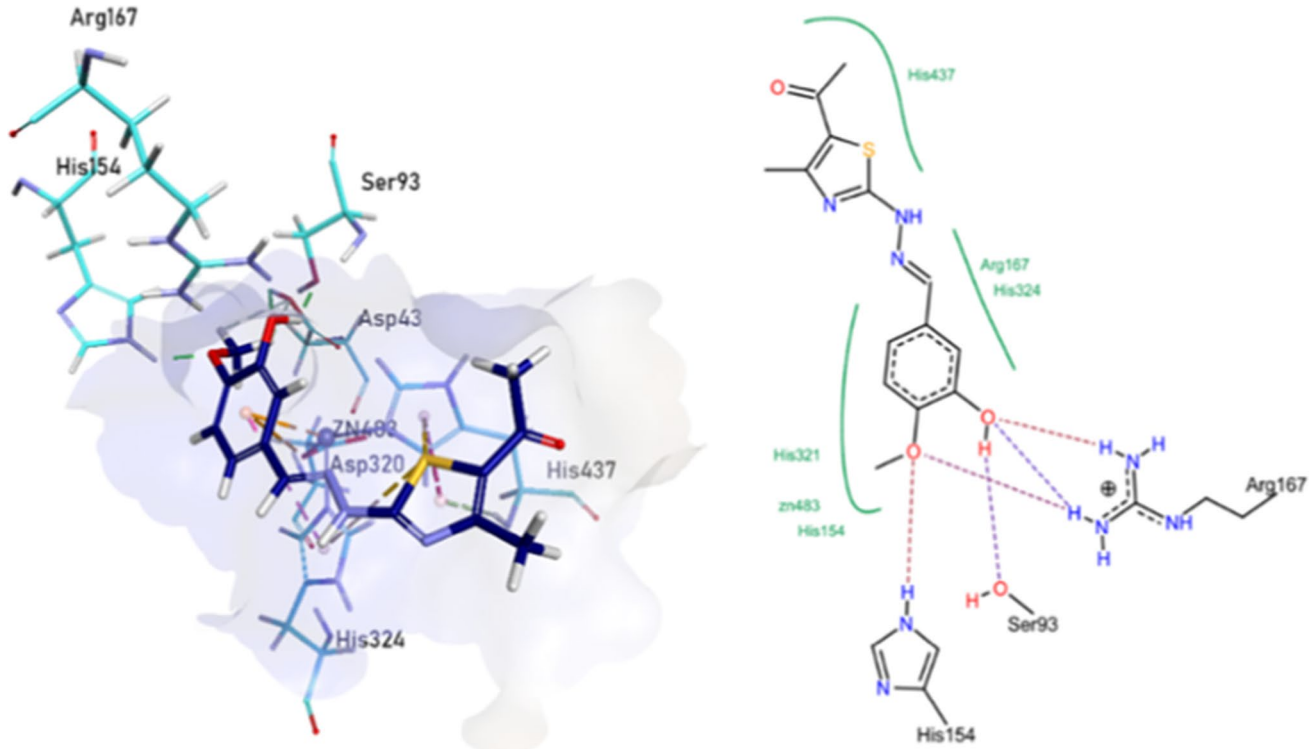

Fig. 7 Compound **3c** docking with h-TNAP

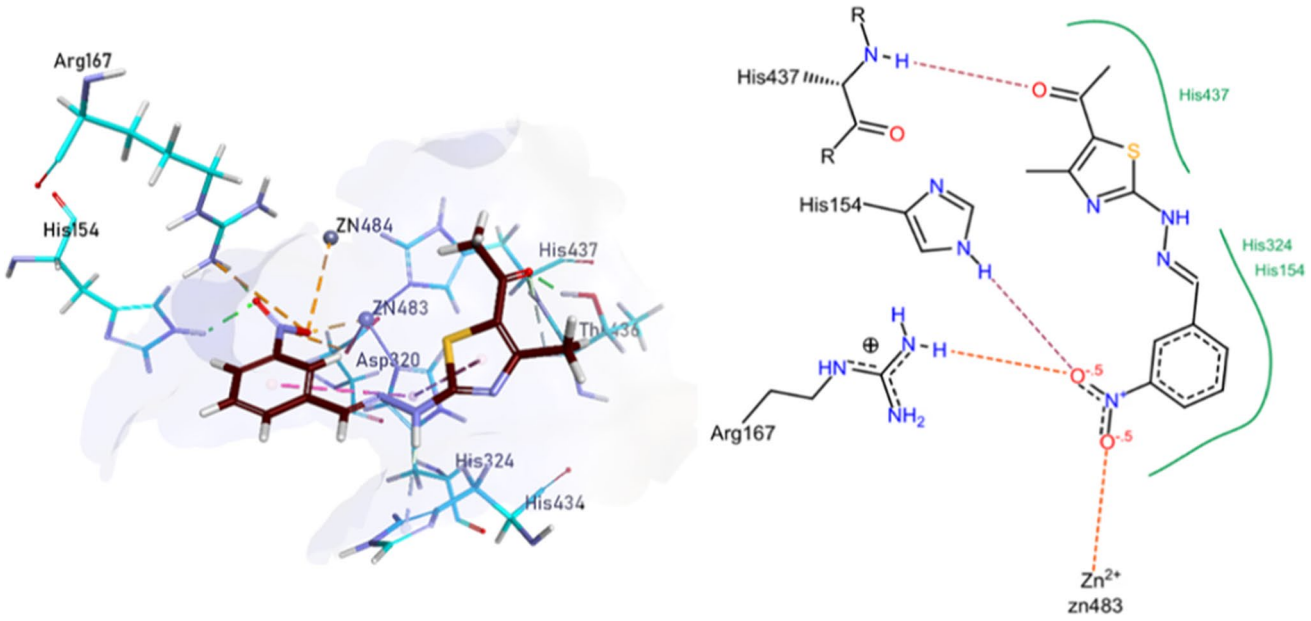

Fig. 8 Compound **3f** docking with h-TNAP

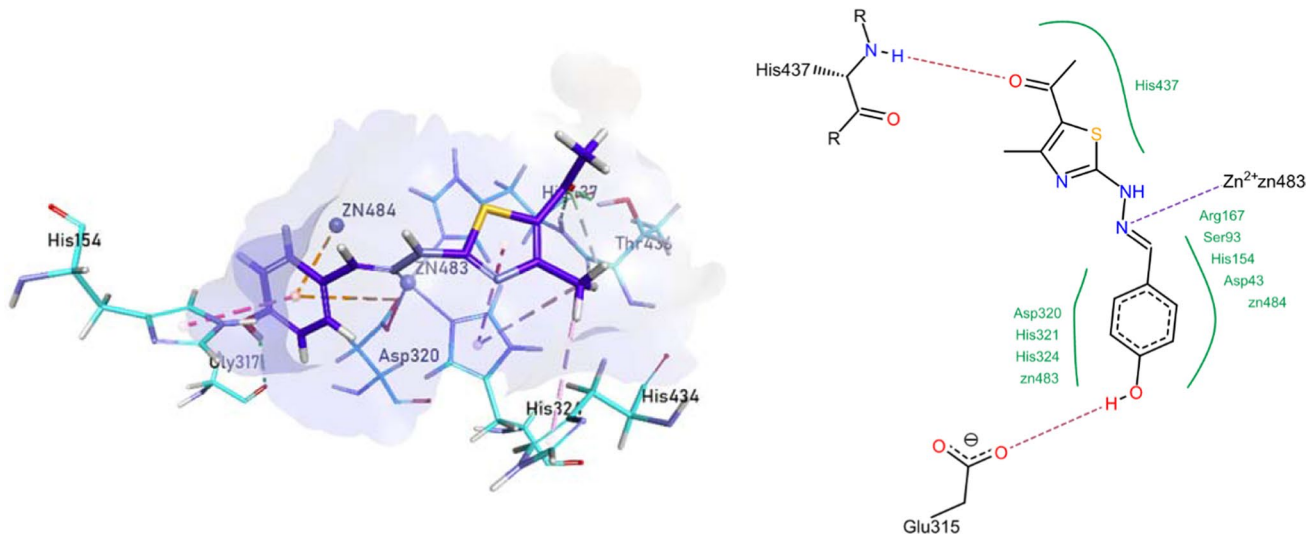

Fig. 9 Compound **3g** docking with h-TNAP

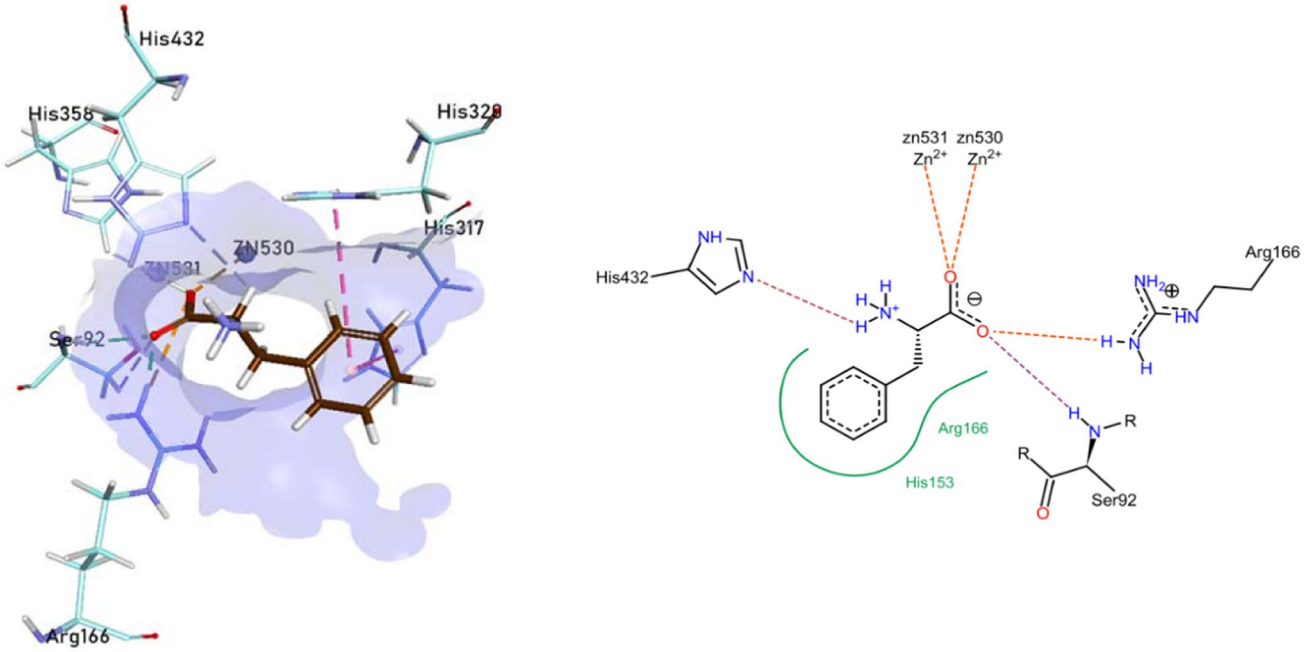

Fig. 10 L-phenylalanine docking with h-IAP

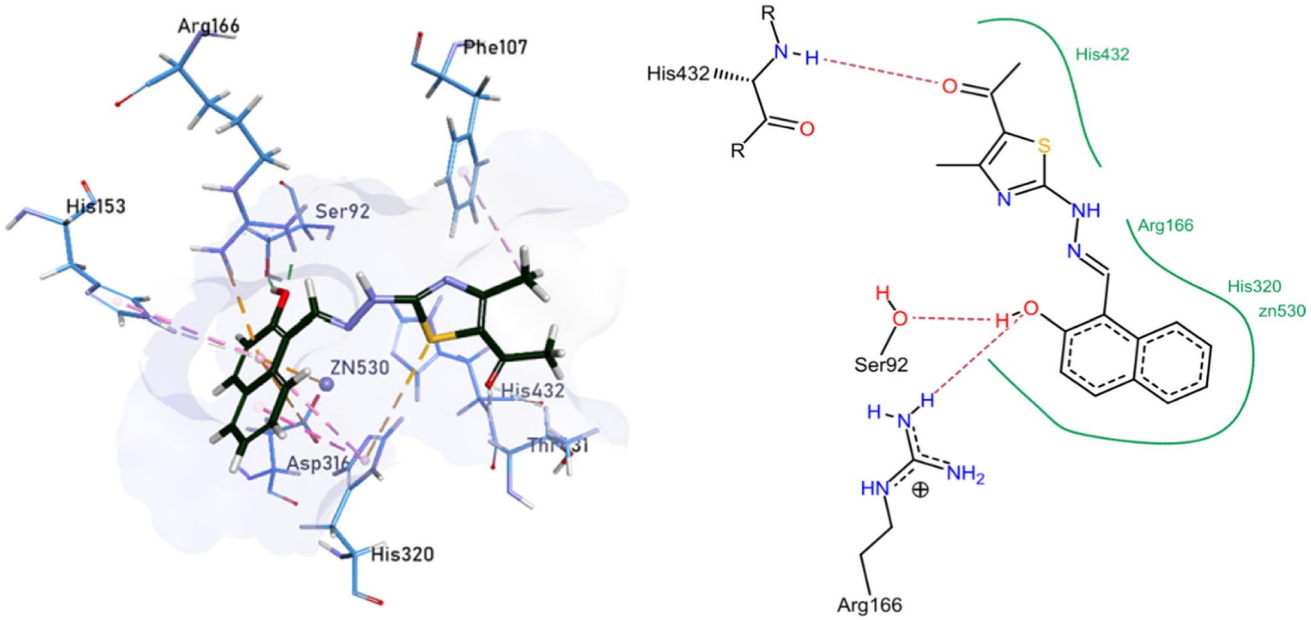

Fig. 11 Compound **3a** docking with h-IAP

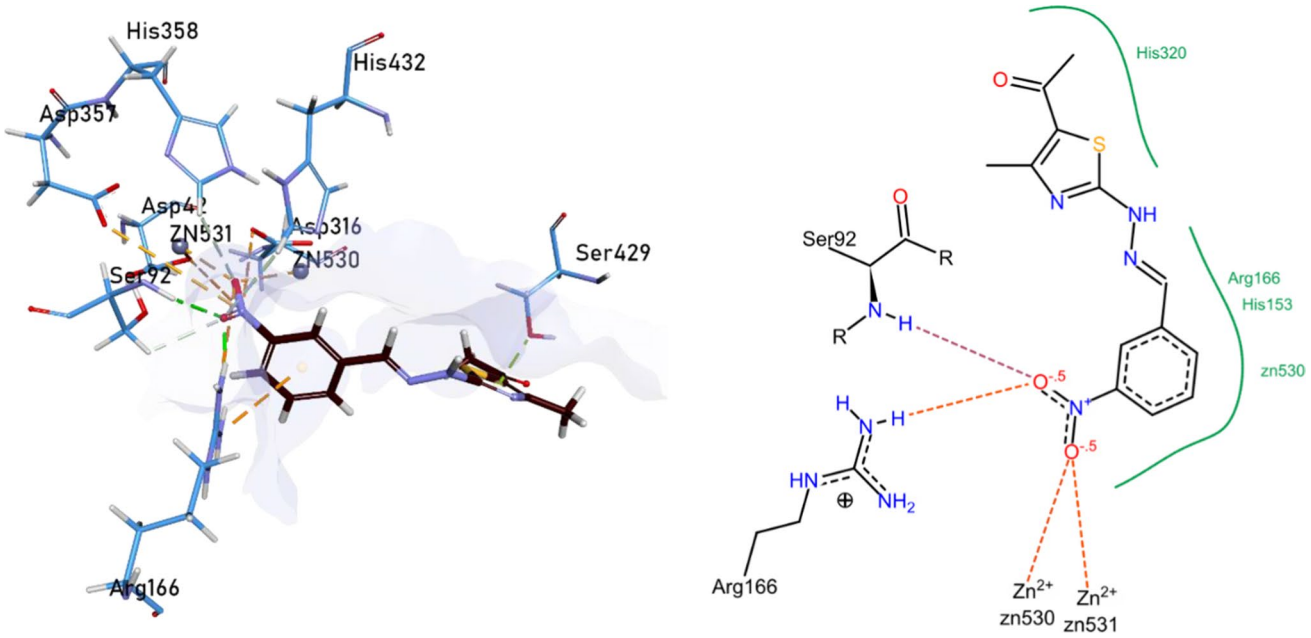

Fig. 12 Compound **3f** docking with h-IAP

docking studies which revealed significant binding interactions between the selected compounds and enzyme active pockets. Such interactions provided further confirmation of in vitro analysis.

Table 2 Docking scores of compounds (3a–3i)

Compound	Highest docking score	
	TNAP	IAP
3a	−15.65	−20.99
3b	−14.09	−18.34
3c	−17.56	−20.56
3d	−15.74	−18.79
3e	−14.52	−24.10
3f	−21.02	−26.72
3g	−14.26	−16.84
3h	−15.66	−16.61
3i	−16.33	−18.72
Levamisole	−12.08	–
L-Phenylalanine	–	−13.07

Acknowledgements Authors are thankful to the Higher Education Commission of Pakistan for the financial support.

Declarations

Competing interest The authors declare no competing interests.

Ethics Approval and Consent to Participate This article does not contain any studies with human participants or animals performed by any of the authors. All the authors have given consent to participate in the manuscript.

Consent for Publication All the authors have given consent for the publication of the manuscript.

References

1. Sharma U, Pal D, Prasad R (2014) Alkaline phosphatase: an overview. Indian J Clin Biochem 29(3):269–278
2. Salar U, Khan KM, Iqbal J, Ejaz SA, Hameed A, Al-Rashida M, Parveen S, Tahir MN (2017) Coumarin sulfonates: new alkaline phosphatase inhibitors; in vitro and in silico studies. Eur J Med Chem 131:29–47
3. Díez-Zaera M, Díaz-Hernández JI, Hernández-Álvarez E, Zimmermann H, Díaz-Hernández M, Miras-Portugal MT (2011) Tissue-nonspecific alkaline phosphatase promotes axonal growth of hippocampal neurons. Mol Biol Cell 22(7):1014–1024

4. Sebastián-Serrano Á, Diego-García D, Díaz-Hernández M (2018) The neurotoxic role of extracellular tau protein. Int J Mol Sci 19(4):998
5. Tsai LC, Hung MW, Chen YH, Su WC, Chang GG, Chang TC (2000) Expression and regulation of alkaline phosphatases in human breast cancer MCF-7 cells. Eur J Biochem 267(5):1330–1339
6. Whyte MP (2010) Physiological role of alkaline phosphatase explored in hypophosphatasia. Ann N Y Acad Sci 1192(1):190–200
7. Kellett KA, Hooper NM (2015) The role of tissue non-specific alkaline phosphatase (TNAP) in neurodegenerative diseases: Alzheimer's disease in the focus. In: Neuronal Tissue-Nonspecific Alkaline Phosphatase (TNAP). Springer, Dordrecht, pp 363–374.
8. Schiele F, Vincent-Viry M, Fournier B, Starck M, Siest G (1998) Biological effects of eleven combined oral contraceptives on serum triglycerides, γ-glutamyltransferase, alkaline phosphatase, bilirubin and other biochemical variables. Clin Chem Lab Med 36(11):871–878
9. Sun Y, Hanley EN Jr (2007) Calcium-containing crystals and osteoarthritis. Curr Opin Orthop 18(5):472–478
10. Derfus BA, Kurian JB, Butler JJ, Daft LJ, Carrera GF, Ryan LM, Rosenthal AK (2002) The high prevalence of pathologic calcium crystals in pre-operative knees. J Rheumatol 29(3):570–574
11. Li L, Chang L, Pellet-Rostaing S, Liger F, Lemaire M, Buchet R, Wu Y (2009) Synthesis and evaluation of benzo [*b*] thiophene derivatives as inhibitors of alkaline phosphatases. Bioorg Med Chem 17(20):7290–7300
12. Chang L, Mébarek S, Popowycz F, Pellet-Rostaing S, Lemaire M, Buchet R (2011) Synthesis and evaluation of thiophenyl derivatives as inhibitors of alkaline phosphatase. Bioorg Med Chem Lett 21(8):2297–2301
13. Channar PA, Irum H, Mahmood A, Shabir G, Zaib S, Saeed A, Ashraf Z, Larik FA, Lecka J, Sevigny J, Iqbal J (2019) Design, synthesis and biological evaluation of trinary benzocoumarin-thiazoles-azomethines derivatives as effective and selective inhibitors of alkaline phosphatase. Bioorganic Chem 91:103137.
14. Iqbal J, Ejaz SA, Ibrar A, Umar MI, Lecka J, Sévigny J, Saeed A (2018) Expanding the alkaline phosphatase inhibition, cytotoxic and proapoptotic profile of Biscoumarin-Iminothiazole and Coumarin-Triazolothiadiazine conjugates. Chemistry Select 3(47):13377–13386
15. Singh M, Yadav VB, Ansari MD, Manisha Malviya, Siddiqui IR (2021) Efficient one-pot synthesis of substituted diphenyl 1, 3-thiazole through multicomponent reaction by using green and efficient Iron-catalyst via Cross-Dehydrogenative Coupling (CDC). Mol Divers.
16. Hassan AU, Sumrra SH, Zafar MN, Nazar MF, Ehsan Ullah Mughal EU (2021) New organosulfur metallic compounds as potent drugs: synthesis, molecular modeling, spectral, antimicrobial, drug likeness and DFT analysis. Mol Divers.
17. Bravo Y, Teriete P, Dhanya RP, Dahl R, San Lee P, Kiffer-Moreira S, Reddy Ganji S, Eduard S, Layton HS, Colin F, Millán JL, Nicholas DPC (2014) Design, synthesis, and evaluation of benzoisothiazolones as selective inhibitors of PHOSPHO1. Bioorg Med Chem Lett 24(17):4308–4311
18. Kukulski F, Lévesque SA, Lavoie EG, Lecka J, Bigonnesse F, Knowles AF, Robson SC, Kirley TL, Sévigny J (2005) Comparative hydrolysis of P2 receptor agonists by NTPDases 1, 2, 3 and 8. Purinergic Signal 1(2):193
19. Nai Yuan Chen, Yu Lan Xie, Guo Dong Lu, Fang Ye, Xin Yu Li, Yu Wen Huang, Ming Li Huang, Tie Yu Chen, Cui Ping L (2021) Synthesis and antitumor evaluation of (aryl)methyl-amine derivatives of dehydroabietic acid-based B ring-fused-thiazole as potential PI3K/AKT/mTOR signaling pathway inhibitors. Mol Divers 25:967–979
20. Channar PA, Irum H, Mahmood A, Shabir G, Zaib S, Saeed A, Ashraf Z, Ali Larik F, Lecka J, Sévigny J, Jamshed Iqbal J (2019) Design, synthesis and biological evaluation of trinary benzocoumarinthiazoles-azomethines derivatives as effective and selective inhibitors of alkaline phosphatase. Bioorganic Chem 91:103137.
21. Chemical Computing Group's Molecular Operating Environment (MOE) MOE 2019.0201.
22. LeadIT version 2.3.2; BioSolveIT GmbH, Sankt Augustin, Germany, 2017, www.biosolveit.de/LeadIT
23. BIOVIA Discovery Studio Client v19.1.0.18287